Glomerular Permeability Barrier in the Rat

Functional Assessment by In Vitro Methods

Barbara S. Daniels,* William M. Deen,‡ Gert Mayer,§ Timothy Meyer,§ and Thomas H. Hostetter*

**Department of Medicine, University of Minnesota, Minneapolis, Minnesota 55455; ‡Department of Chemical Engineering, Massachusetts Institute of Technology, Cambridge, Massachusetts 02139; §Department of Medicine, Stanford University, Stanford, California 94305*

Abstract

The formation of glomerular ultrafiltrate is dependent on the prevailing hemodynamic forces within the glomerular microcirculation and the intrinsic properties of the filtration barrier. However, direct assessment of the permeability barrier is difficult with most available techniques. We used confocal microscopy to image 1-μm thick optical cross-sections of isolated intact glomeruli and glomeruli denuded of cells and quantitated dextran (70,000 mol wt) diffusion from the capillary lumen. Dextran permeance was 11 times greater for the acellular filtration barrier than the intact peripheral capillary. Consideration of the basement membrane and cells as series resistors demonstrated that cells of the filtration barrier contribute 90% of the total resistance to macromolecular permeance. Using a different approach, dextran sieving coefficients for acellular glomeruli consolidated as a multilayer sheet in a filtration cell were similar to those for intact glomeruli in vivo at radii 30–36 Å and ~ 50 times greater at a dextran radius of 60 Å. The presence of cells significantly reduced hydraulic permeability determined on consolidated intact or acellular glomeruli in an ultrafiltration cell with 50 mmHg applied pressure. The glomerular basement membrane does restrict macromolecular permeability but cells are important determinants of the overall macromolecular and hydraulic permeability of the glomerulus. (*J. Clin. Invest.* 1993. 92:929–936.) Key words: permeability • glomerulus • glomerular epithelial cells • permselectivity

Introduction

The formation of ultrafiltrate by the glomerulus is dependent on both the prevailing hemodynamic forces within the glomerular microcirculation and the intrinsic properties of the glomerular permeability barrier (1–3). Alterations in glomerular capillary pressures and flow rates result in well described changes in the glomerular filtration rate and macromolecular clearance. However, investigation of intrinsic glomerular capillary wall function is most often confined to either the calculation of the glomerular ultrafiltration coefficient (K_f)[1] from micropuncture data (4, 5) or modeled membrane pore parameters, such as the shunt pathway or pore radius from dextran sieving studies (6, 7). While those methodologies have provided important insights into glomerular barrier function, it is often impossible to differentiate the effects of hemodynamic and hormonal influences from those properties intrinsic to the filter. In addition, determination of the contribution of each layer of the filter to the overall permeability properties of the glomerulus has been difficult. An understanding of the contributions of the various layers of the filtration barrier to the overall permeability properties of the glomerulus would be of value in understanding the structural and cellular basis of proteinuria and for developing new strategies to ameliorate proteinuria and its consequences by targeting appropriate sites within the filtration barrier.

To examine these issues, we developed a method whereby the diffusion of fluorescent macromolecules across individual glomerular capillaries could be assessed in thin optical cross sections of intact glomeruli by confocal microscopy. The studies described herein represent the first application of this methodology to glomerular function. We were able to determine the relative contribution of cells and the glomerular basement membrane to the overall permeability properties of the glomerulus. We also determined the size-selective properties of acellular glomeruli in vitro and glomeruli in vivo. Finally, we assessed hydraulic conductivity of consolidated layers of cellular or acellular glomeruli in a filtration cell.

Methods

Isolation of glomeruli

Male Sprague Dawley rats weighing ~ 350 g (Harlan Sprague Dawley, Inc., Indianapolis, IN) were anesthetized with Inactin (100 mg/kg body wt) and kidneys were perfused in situ at 110 mmHg with modified Eagle's medium (pH 7.4) to remove blood. Perfusion was usually complete within 10 s. Cortex was minced and glomeruli were isolated by differential sieving. The isolation procedure was accomplished on ice in the presence of buffer with 5 mM pyruvate, 5 mM butyrate, and 1 mM alanine, and resulted in a preparation with > 95% glomeruli < 5% tubular fragments as assessed by light microscopy. More than 95% of the glomeruli were free of Bowman's capsule (8).

Preparation of acellular glomeruli

Acellular glomeruli were prepared according to the method of Ligler and Robinson (9) as previously applied in our laboratory (8). Briefly, glomeruli were incubated with *N*-lauryl sarcosine to lyse cells and DNAse to remove nucleoprotein. The residual glomerular "skeletons" maintained the general shape of the glomerulus, as previously reported by others (10), and consisted primarily of glomerular basement membrane (GBM) with areas of residual mesangial matrix. As previously described, GBM obtained in this manner in our laboratory retains immunofluorescence for type IV collagen, heparan sulfate proteoglycan, laminin, and fibronectin (8).

Address correspondence to Barbara S. Daniels, M.D., Department of Medicine, Box 736 UMHC, University of Minnesota, Minneapolis, MN 55455.

Received for publication 10 August 1992 and in revised form 23 March 1993.

1. *Abbreviation used in this paper: GBM, glomerular basement membrane.*

J. Clin. Invest.

0021-9738/93/08/0929/08 $2.00
Volume 92, August 1993, 929–936

Confocal microscope

A fluorescent cell analysis system (model ACAS 570; Meridian Instruments Inc., Okemos, MI) modified by the manufacturer for confocal microscopy was used. A 5-W Argon laser (Coherent Inova 90-5) was used as the fluorescence excitation source. An Olympus epifluorescence inverted microscope was equipped with a precision gear to provide measured alterations in the z axis. Either phase contrast or fluorescent images could be obtained. A pinhole limited the entrance of light to the photodetector to that originating from within the plane of focus and was adjustable to facilitate variations of optical section thickness. For the present studies, a pinhole of 225 μm was used to produce section thickness of $\sim$ 1 μm. A 30 $\times$ 30-μm area was scanned at a step size of 0.4 μm, a peak velocity of 0.4 mm/s with a laser power of $\sim$ 3 mW. Each point was sampled eight times, the first time for 8 μs and subsequent samplings for 4 μs so that the total laser exposure time was 36 μs. Approximately 30% of the laser power is present in the 488-nm line so that 0.9 mW of laser power was transmitted to the sample. All laser parameters were set to limit sample photobleaching to < 5% loss of the initial fluorescence per 100 scans. Images were stored digitally on Bernoulli disks and were subsequently analyzed with image analysis software integral to the ACAS system.

Permeability determinations with confocal microscopy

Intact or acellular glomeruli were incubated at 27°C for 20 min in fluoresceinated dextran 70,000 mol wt (2 mg/ml) (Molecular Probes, Inc., Eugene, Oregon) in DME (25 mM Hepes) buffer with 5 mM butyrate, 5 mM alanine, and 5 mM pyruvate substituted for equimolar NaCl. This resulted in diffusion of the dextran from the bath into the capillary lumen. Glomeruli were then placed in a coverglass chamber (Nunc Inc., Naperville, IL) and immobilized with weighted nylon mesh to minimize movement during the scans. A longitudinal section of glomerular capillary without an overlying epithelial cell body was located by phase contrast microscopy and a plane of focus through the maximal diameter of the capillary was selected for ease in repeated identification of the original plane of focus. An initial fluorescent scan was then obtained to quantitate intracapillary fluorescence. The background fluorescence was rapidly decreased (over a couple of seconds) by removing $\sim$ 75% of the fluorescent buffer and adding fresh buffer devoid of fluoresceinated dextran. Although the actual buffer exchange could be accomplished in $\sim$ 5 s, the first scan was delayed by $\leq$ 120 s to confirm the original plane of focus. Because the diffusion of dextran was very rapid across acellular glomeruli, only glomeruli that did not move were used for those studies. The decline in fluorescence within the capillary was then serially assessed by obtaining confocal images every 20–40 s. The bath fluorescence usually remained constant because of its large volume relative to intraglomerular or intracapillary volume. For occassional glomeruli, background fluorescence increased, probably because of leakage of fluorescence from the vascular pole and such glomeruli were excluded from further analysis. The mean pixel fluorescence for an intracapillary area $\sim$ 5 $\times$ 4 μm and adjacent to the capillary wall and for an similar sized area in the bath adjacent to the capillary was quantitated with image analysis software integral to the ACAS system.

Filtration cell

Acellular (150 μg protein) or intact glomeruli (600 μg protein consisting of 100 μg "GBM" protein) were consolidated in a modified miniultrafiltration cell (model 3; Amicon, Beverly, MA). Acellular glomeruli were consolidated as previously described (8), except that DME (pH 7.4) with 5 mM pyruvate, 5 mM butyrate, and 1 mM alanine substituted for equimolar amounts of sodium chloride. Intact glomeruli were consolidated in an analagous manner. The GBM or glomeruli form a uniform filter at the base of the cell as was evidenced by light microscopy. In addition, when filters of glomeruli were exposed to the vital dye dicarboxyfluorescein diacetate (Molecular Probes, Inc., Eugene, OR) at the completion of the filtration studies, fluorescence was homogeneous across the filter, evidence of the viability of the glomeruli at the completion of the studies, as well as the uniformity of glomerular layering. Glomeruli monitored by phase contrast confocal microscopy for a similar time period under identical conditions retained normal epithelial cell morphology. After consolidation, the buffer was removed and replaced with identical buffer containing 4 g/dl bovine serum albumin. Filtration studies were conducted at 50 mmHg applied pressure to approximate the in vivo glomerular capillary hydrostatic pressure and 27°C. After a 10-min equilibration, the filtrate was collected for either 15 or 20 min. The retentate was sampled at the start and completion of each clearance period. Preliminary studies demonstrated that when similar numbers of acellular and intact glomeruli were used to form the filter the rate of water flux was slow and the duration of time needed for an adequate collection of filtrate was longer than optimal for maintaining the viability of the glomeruli. Therefore, the quantity of intact glomeruli used was decreased, such that 600 μg glomerular protein containing 100 μg "acellular" glomerular protein was used to form the filters of consolidated glomeruli. We have estimated that the filters of acellular glomeruli were comprised of 40 layers (8) and, based on the difference in protein quantity, intact glomerular filters have 27 layers.

Dextran sieving

Polydisperse dextran (1 mg/ml T40 and 1 mg/ml T70) in rat plasma was added to the filtration cell and, after a 20-min equilibration period, the retentate was sampled at the midpoint, and the filtrate was collected throughout of a 20-min clearance period.

Calculations

Diffusion model for isolated glomeruli. The capillary lumen and the bath (corresponding to Bowman's space in vivo) were taken as well-mixed compartments separated by a membrane of surface area A. Given that the solute concentration in the bath (C_B) was found to remain constant during the period of observation, a mass balance equation was needed only for the luminal compartment (concentration C_L and volume V_L). The mass balance was written as:

$$\frac{dC_L}{dt} = -\frac{k_s A}{V_L}(C_L - C_B), \tag{1}$$

where k_s is the diffusional permeability of the capillary wall to the test solute, a mass transfer coefficient. The solution to equation 1 indicates that $\Delta C = C_L - C_B$ decays with time according to

$$\Delta C = C_0 \exp\left[-\frac{k_s A}{V_L} t\right], \tag{2}$$

where C_0 is the initial value of ΔC. For observations on a capillary segment of radius R and length L, $A/V_L = (2\pi RL)/(\pi R^2 L) = 2/R$. Making this substitution, equation 2 can be rewritten as:

$$-\ln\frac{\Delta C}{C_0} = \left(\frac{2k_s}{R}\right)\cdot t. \tag{3}$$

Thus, a plot of $\ln(\Delta C/C_0)$ vs t has a slope of $2k_s/R$, allowing k_s to be determined from the observed slope and the capillary radius. Capillary radius was determined using image analysis software integral to the ACAS system.

To determine the mass transfer coefficient for the movement of dextran through a hypothetical aqueous "membrane," k_a, the following relationship was used

$$k_a = \frac{D_\infty}{l}, \tag{4}$$

where l is the thickness of the aqueous membrane (selected as 200 nm

to approximate the thickness of the glomerular basement membrane), and D_∞ is the diffusivity of dextran at 27°C in a dilute aqueous solution. For 70,000 mol wt dextran, D_∞ is 4.0×10^{-7} cm^2/s (11), giving k_a as 2.0×10^{-2} cm/s.

To determine the relative contribution of the GBM and cells of the peripheral capillary to the macromolecular diffusional permeability of the filtration barrier, the filtration barrier was taken as a membrane with the GBM and cells functioning as resistors in series. Mass transfer coefficients represent the reciprocal of resistance so that:

$$\frac{1}{k_{GBM}} + \frac{1}{k_{cells}} = \frac{1}{k_G}, \quad (5)$$

where k_{GBM} represents the mass transfer coefficient for GBM, k_{cells} is the mass transfer coefficient for the cellular component of the filtration barrier, and k_G represents mass transfer across the intact glomerular capillary wall.

Sieving coefficients for studies in the filtration cell were calculated as we have previously described. Briefly,

$$\theta' = \frac{C_F}{C_R}, \quad (6)$$

where θ' is the measured sieving coefficient, C_F is the filtrate concentration of dextran, and C_R is the corresponding concentration in the bulk retentate. Membrane sieving coefficients (θ) are defined by

$$\theta = \frac{C_F}{C_M}, \quad (7)$$

where C_M is the concentration on the retentate side immediately adjacent to the membrane surface. The difference in C_M and C_R is caused by concentration polarization at the membrane surface. θ is related to θ' by the following relationship:

$$\theta = \frac{\theta'}{(1 - \theta')B + \theta'}, \quad (8)$$

where B is the polarization factor described by the relationship $B = \exp(J_v/k_c)$ where J_v is the volume flux in centimeters per second, and k_c is the mass transfer coefficient previously determined for these experimental conditions (8).

Hydraulic conductivity. Hydraulic conductivity (L_p) was calculated as

$$L_p = J_v/(\Delta P - \Delta\Pi), \quad (9)$$

where J_v is the volume flow rate in centimeters per second, ΔP is the applied hydrostatic pressure gradient in mmHg, and $\Delta\Pi$ is the oncotic pressure gradient in millimeters of mercury calculated from C_M and C_F for albumin as we have previously described (8). To estimate the hydraulic conductivity of a single layer, each filter was considered to comprise many layers functioning as resistors in series.

$$L_p^1 = N(L_p), \quad (10)$$

where N is the number of layers in the filter. N was previously estimated as 40 for the acellular glomerular (GBM) filters (8). Because one third less GBM protein was present in the intact glomerular filters, N was estimated as 27 for those filters.

Dextran separation. Filtrate and retentate samples were deproteinized in 0.5 N NaOH and 10% zinc sulfate, centrifuged, filtered, and the supernatant was subjected to gel filtration chromatography using an HPLC system with Ultrahydrogel 250 and Ultrahydrogel 500 columns in series as previously described (12, 13, 14). A refractive index detector was used to quantitate dextran concentration in each 2-Å size fraction.

The diffusivity for each 2-Å dextran fraction (D_∞) was determined from its Stokes-Einstein radius (r_s):

$$D_\infty = \frac{\kappa T}{6\pi\eta r_s}$$

where κ = Boltzmann's constant, T = absolute temperature, and η = viscosity of water at 27°C. The polarization factor (B) was then calculated as above for each dextran fraction, and the sieving coefficient for each 2-Å fraction was calculated as we have previously described (8).

Assays

Protein was determined by the Coomasie assay.

Statistics

Results are mean±SE. Student's t tests were used to assess statistical significance. $P < 0.05$ was taken as significant and all significant P values are expressed as such regardless of their absolute value.

Results

Epithelial foot processes and endothelial fenestrae were present on the glomerular capillary after the isolation procedure. Epithelial cell fluorescence after exposure to the dye dicarboxyfluorescein diacetate, a marker of cell vitality, was preserved throughout the duration of the studies. Also, epithelial cell morphology by phase contrast microscopy on the ACAS 570 system remained constant, without apparent blebbing or swelling.

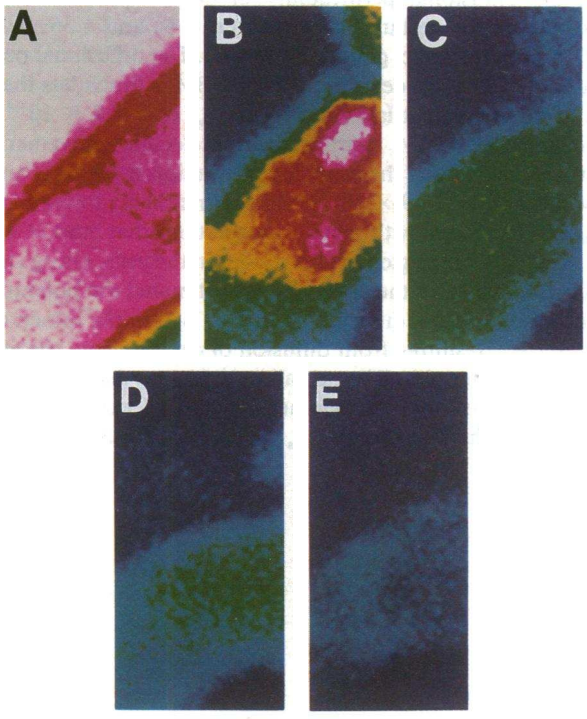

Figure 1. Diffusion of fluoresceinated dextran from the glomerular capillary lumen. (*A*) Baseline scan. Glomerulus were incubated with fluoresceinated dextran resulting in diffusion of dextran from the bath (Bowman's space) to the capillary lumen. (*B*) 100 s. The background fluorescence was removed and the diffusion of dextran from the lumen to the bath was determined. The low level of fluorescence is represented by blue while increasing levels of fluorescence are shown as green, yellow, red, pink, and white. (*C*) 160 s. Dextran fluorescence within the capillary lumen has decreased. Background fluorescence remains relatively constant because of the large volume of the bath relative to the glomerulus. (*D*) 220 s. (*E*) 280 s.

Intact or acellular glomeruli were incubated in fluoresceinated dextran (70,000 mol wt) at a concentration of 2 mg/ml to effect diffusion of the macromolecule into the capillary lumen. After an initial scan (Fig. 1 *A*), the background fluorescence was reduced and the diffusion of dextran from the capillary lumen to the bath was monitored with serial confocal images obtained every 20–40 s until equilibration across the capillary wall occurred, as shown in Fig. 1, *B–D*. A plot of intracapillary fluorescence vs time for a single representative glomerulus is shown in Fig. 2. The fluorescence of the bath, which is analogous to Bowman's space is represented by the lower curve. The bath fluorescence typically remained constant, probably because of its large volume relative to that of the glomerular capillaries.

To assess the relative contributions of GBM and glomerular cells to the permeability properties of the glomerulus, glomeruli were studied in either their intact state or after detergent lysis to remove cells, resulting in glomerular skeletons that retain their spherical shape, as well as outlines of capillaries. The filtration surface in intact glomeruli consists of epithelial and endothelial cells, as well as basement membrane, while the filtration surface in acellular glomeruli is solely GBM. The rate of decline in fluorescence per second is shown in Fig. 3 for a representative study from each group. From the slopes of these plots for each glomerulus studied and the measured capillary radii the diffusional permeability of GBM was 15.5±0.05 $\times 10^{-6}$ cm/s for acellular glomeruli (n = 6) and 1.36±0.05 $\times 10^{-6}$ cm/s for intact glomeruli (n = 6). The diffusional permeability of this size dextran through GBM is much less than that of an equivalent layer of H_2) ($k_{GBM}/k_a = 7.8 \times 10^{-4}$), indicating that GBM restricts macromolecular movement. However, calculating the cellular contribution from k_{GBM} and k_G yields k_{cells} of 1.49×10^{-6}, which is markedly lower than k_{GBM} and consistent with previous suggestions that most of the size selectivity of the glomerulus resides in the cells. Using calculations detailed in the appendix, we estimated the potential contribution of axial diffusion of dextran within the lumen of the capillary, resulting from diffusion of dextran from the cut ends of the arterioles. The actual k_s (k_s*) may have been as much as 11% less for intact glomeruli and 0.1% less for acellular glomeruli than the observed k_s. Thus, axial diffusion cannot account for the very large difference between the observed k_s for intact and acellular glomeruli.

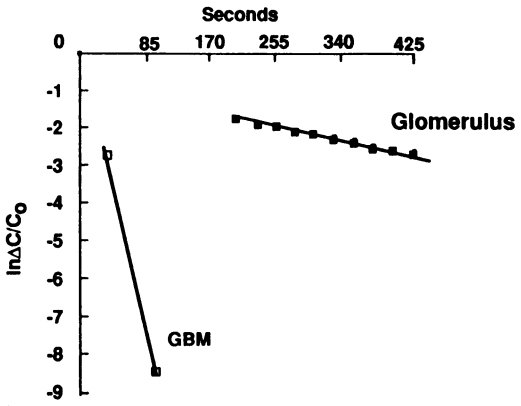

Figure 3. Plot of the decline in fluorescence. The ratio ln $\Delta C/C_0$ represents the difference in fluorescence across the capillary wall (ΔC) relative to the initial difference in fluorescence (C_0). This plot of ln $\Delta C/C_0$ vs. time for a representative intact glomerulus and acellular glomerulus (*GBM*). The slope is proportional to k_s.

To further assess the contribution of the glomerular cells to the size selectivity of the glomerulus, dextran sieving curves for acellular glomeruli in vitro were compared with those obtained for the rat glomerulus in vivo. The polarization factor B for each 2-Å dextran fraction varied from 1.13 for 32 Å to 1.23 for 70 Å. As shown in Fig. 4, the sieving coefficient of each dextran fraction decreases with increasing molecular radius demonstrating size selectivity of the GBM. For comparison, data obtained previously by Mayer et al. for the rat glomerulus in vivo (12) and analyzed by identical methods are also shown. At radii < 36 Å the two curves are remarkably similar. For example, at 34 Å, θ is 0.40 for both GBM and the in vivo glomerulus. However, differences in permeability between acellular and intact glomeruli in vivo become more apparent with progressive increments in dextran size so that at a dextran radius of 70 Å, θ is 0.013±0.001 for acellular GBM and 0.0063±0.0007 in vivo. Thus, the contribution of the cells to the overall permselectivity properties of the glomerulus is most conspicuous at the largest molecular radii.

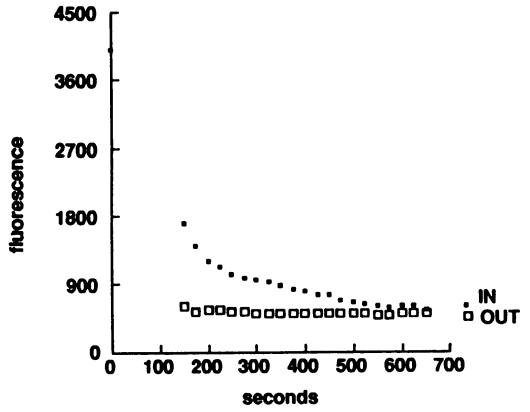

Figure 2. Plot of decline in fluorescence with time. Solid squares represent fluorescence within the capillary (*IN*) and open squares represent bath fluorescence (*OUT*). The exponential decline in capillary lumen fluorescence is apparent.

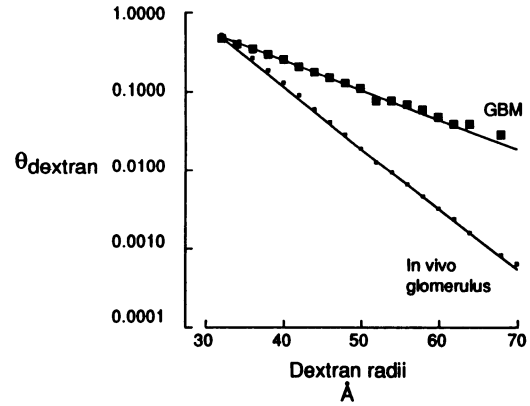

Figure 4. Dextran sieving curves for GBM (n = 6) and the in vivo glomerulus (n = 16). θ_D represents the sieving coefficient for dextran at each molecular radius.

The filtration cell allowed us to measure the hydraulic conductivity for consolidated and intact glomeruli. Filters of acellular glomeruli exhibited greater hydraulic conductivity than intact glomeruli (4.24±0.28 vs 1.46±0.05 cm/s per mmHg $\times 10^{-6}$; acellular vs intact glomeruli; $P < 0.05$). When estimated per layer of glomerular filtration surface, the differences between acellular and intact glomeruli are more pronounced (Fig. 5). Thus, these studies offer evidence that the cells of the glomerulus contribute importantly to the hydraulic permeability properties of the glomerulus.

Discussion

The relative contribution of the highly differentiated endothelial and epithelial cells and the structurally unique basement membrane to the permeability properties of the glomerulus has been the center of much debate, but available technology has been inadequate to resolve the controversy. In vivo studies can define the integrated function of the glomerulus but can neither differentiate hemodynamic and hormonal effects from intrinsic barrier function nor assess the relative contribution of the components of the capillary wall. Although glomerular cell culture techniques have contributed to the understanding of other areas of glomerular function, their contribution to understanding glomerular permselectivity has been limited because epithelial cells in culture typically do not retain foot processes, endothelial cells do not faithfully retain fenestrae, and reassembly of two or more components has yet to be accomplished. The role of the glomerular basement membrane in restricting permeance of macromolecules has been emphasized for nearly two decades (15–17). However, many previous studies localizing GBM as the principal site of permselectivity within the filtration barrier have been qualitative and relied on visual localization of the restriction of electron dense tracers within the GBM in fixed tissue (15, 16, reviewed in reference 17). We and others, based on permeability determinations of GBM (8, 16) or renal cortical basement membranes (19) in a filtration cell, have previously expressed doubt as to the exclusive nature of the GBM in restricting macromolecular permeability through the glomerulus. However, available techniques have not quantitatively and dynamically allowed functional dissection of the filtration barrier.

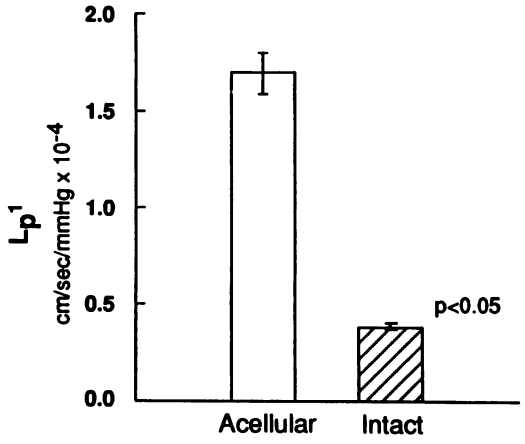

Figure 5. Hydraulic conductivity (L_p) for acellular ($n = 8$) and intact glomeruli ($n = 8$) determined in the filtration cell.

The development of the confocal methodology for assessing glomerular permeability to macromolecules together with the mathematical construction of the diffusion model of the isolated glomerulus provide advantages complementary to the filtration cell and in vivo studies. First, the anatomically normal structure is studied with macromolecule flux directed from lumen to bath (Bowman's space) rather than the compacted structures with bidirectional flux studied in the filtration cell. A purely diffusional flux is observed in the confocal approach without contribution of hemodynamic forces. On the other hand, the filtration cell method measures macromolecule flux caused by convective, as well as diffusive movement, a circumstance more similar to the in vivo situation. Also, the filtration cell reflects the composite effects of many glomeruli rather like sieving curves obtained in vivo. Overall, the ability to compare data from all three approaches, confocal, filtration cell and in vivo sieving, allows corroboration of measured and derived parameters, and supplies the clearest quantitative evaluation of the relative roles of cellular and glomerular basement membrane layers across a range of sizes and types of macromolecules.

To quantitate the hindrance provided by GBM with that of the intact capillary, we calculated the mass transfer coefficient for similarly sized dextran across a hypothetical aqueous membrane of a thickness similar to that of the GBM. When compared to an aqueous membrane of similar thickness, the GBM does significantly restrict the diffusional movement of dextran and the presence of cells further limits the permeability of dextran. However, the cells of the glomerular capillary wall are the major site of restriction to macromolecular permeability as indicated by k_{cell} being less than one-tenth that of k_{GBM}.

Comparison of dextran sieving in vivo with that for acellular glomeruli in the filtration cell provides another means of confirmation of the above results. Dextran sieving coefficients for GBM in vitro are remarkably similar to those for intact glomeruli in vivo at lower radii (30–36 Å), but the ratio of GBM to the in vivo θ increases to ten or more at higher radii. In disease states, the greatest abnormalities in dextran permeability are observed at higher molecular radii (13, 14), where our studies suggest that cells of the permeability barrier may provide much of the permselectivity.

In vivo, areas of epithelial cell denudation, possibly analogous to GBM in the present study, are the sites of increased glomerular permeance (20) and the extent of epithelial denudation has been related to proteinuria (21). $\theta_{albumin}$ for the denuded glomerular capillary can be calculated from the morphometric and physiologic data of Miller et al. from studies of rats given adriamycin and subjected to compensatory renal growth after subtotal nephrectomy. If the total peripheral capillary wall is 1.59×10^{-5} μm^2 and filtration occurs by a paracellular route through slit pores, which cover ~ 5% of the peripheral capillary wall (22, 23) then the surface area available for filtration is 7.95×10^{-7} μm^2. The area of denuded GBM was 6.36×10^{-7} μm^2. If hydraulic conductivity were similar for both surfaces, then 31 nl/min would pass through normal peripheral capillary wall and 25 nl/min pass through denuded capillary wall to yield the total measured average single nephron glomerular filtration rate of 56 nl/min. If most of the albumin leakage occurred across areas of denuded GBM, as shown by

Kanwar and Rosenzweig (20), and suggested by Miller et al. (21), then a $\theta_{albumin}$ of 0.15 at the sites of epithelial denudation would be calculated, a value similar to that obtained for GBM in the filtration cell of 0.13±.01 (8). Because cells of the filtration barrier are important in the pathogenesis of proteinuria, strategies to ameliorate cellular abnormalities may provide advances in the treatment of proteinuric renal disease. Given the relatively modest restriction in permeability attributable to the basement membrane, particularly for very large macromolecules, it seems unlikely that strategies targeted directly at the basement membrane would ameliorate proteinuria unless cellular integrity was also enhanced.

The quantitative contribution of each cell type to the overall permeability properties of the filtration barrier cannot be obtained from the present study but available evidence suggests that both epithelial and endothelial cells may contribute. The potential importance of the epithelial cell in glomerular permselectivity is suggested not only by their position as the terminal element in the filtration barrier but also by their unique structure (24, 25). Epithelial cells exhibit highly differentiated foot processes with a well-developed contractile apparatus. Foot processes contain an actin/myosin/α actinin cytoskeleton that is linked to microtubules in the cell body, an arrangement that has been suggested as a mechanism for the regulation of permeability (25). Adjacent foot processes are adjoined by slit pores, a unique type of cell junction with anionic charge covering from 3 to 10% of the GBM area (22, 23). Karnovsky and his coworkers have argued that the slit pores confer permselective properties to the glomerulus (22). As noted above, the presence of increased permeance at the site of epithelial denudation offers additional evidence for the importance of the epithelial cell in glomerular permselectivity. By contrast, glomerular endothelial cells have large fenestrae ($\leq$ 600 Å diameter) which cover up to one third of the capillary surface (26) and are lined by an anionic, sialic acid diaphragm which contains heparan sulfate proteoglycan (27). Although hinderance to macromolecular permeability at glomerular fenestrae has been noted with some electron microscopy tracer studies (15), in general they are not considered a primary site of size restriction because of their very large radii (600 Å), but may be more important in charge selectivity. The location of mesangial cells suggests that they do not directly contribute to glomerular permeability, as they are removed from the principal site of filtration. Small amounts of plasma do percolate through channels present in the mesangium and exit either through lymph or across the mesangium/basement membrane/epithelial cell interface (28). However, this latter surface represents a very small fraction of the visceral filtration surface of the glomerulus.

Despite the considerable hydrostatic pressure within the glomerulus relative to other capillary beds, the actual driving forces for the formation of filtrate are quite small. In the rat, the intraglomerular capillary pressure is $\sim$ 54 mmHg, but the net ultrafiltration pressure is between 5 and 10 mmHg. Thus, relatively large hydraulic conductivity is essential to the maintenance of the glomerular filtration rate. Investigation of intrinsic glomerular capillary wall function is typically confined to the measurement of K_f, the glomerular ultrafiltration coefficient, which is the product of hydraulic conductivity and total capillary surface (4, 5). Water flux through the permeability barrier most likely occurs through a paracellular route. Fenestrated endothelium occurs in organs with high hydraulic conductivity, but it is conspicuously absent in tissues that limit both water and macromolecule permeability, such as the brain (29) and almost certainly facilitates the very high hydraulic conductivity of the glomerular capillary wall. However, the relative contributions of endothelial and epithelial cells in the resistance to water flow remains uncertain, but one would presume that the latter offer the greater share given the relatively smaller area of their intercellular junctions, the slit pores.

These studies use in vitro techniques that do not replicate all of the filtration conditions present in vivo. For the filtration cell, movement of water and macromolecules occurred for lumen to Bowman's space half the time and from Bowman's space to lumen half the time. Such bidirectional movement is obviously different from the in vivo setting, but studies by Landis (30) and Pappenheimer et al. (31) in intact capillaries demonstrate similar hydraulic conductivity regardless of the direction of water movement, and Pinnick and Savin (32) have demonstrated that the Bowman's space to lumen hydraulic conductivity of isolated glomeruli is similar to that for intact glomeruli in vivo. We applied several different in vitro techniques to verify the conclusions and we also compared the resulting measures of permeance with data obtained in vivo. The general agreement of the models presented above, as well as that from calculated results using in vivo data provide support to the view that the models reflect filtration barrier function in vivo.

In conclusion, the present results constitute evidence for roles of both the glomerular basement membrane and the cells of the peripheral capillary wall in maintaining the permselectivity properties of the intact glomerulus. At larger dextran radii, cells of the filtration barrier contribute to permeability properties, while at smaller radii, the GBM accounts for an increasing percentage of the permselectivity.

Appendix

In using equation 3 to calculate macromolecular diffusional permeabilities (k_s) from confocal microscopy data, it is assumed that the decay in luminal concentration (C_L) with time is caused entirely by transmural diffusion of the test molecule. Another factor which might contribute to the observed decline in C_L is luminal diffusion along the length of the capillary, toward the opening at the vascular pole. This will be termed "axial diffusion," to distinguish it from luminal diffusion in the radial direction, toward the capillary wall. Neglecting axial diffusion will tend to overestimate k_s. The relative rates of the processes which diminish C_L are determined by the membrane permeability and the distance of the observation site from the vascular pole: the higher the membrane permeability, and the longer the distance, the less important is axial diffusion. The duration of the experiment is also an important factor. The analysis that follows provides an estimate of the error in the calculated k_s caused by neglecting axial diffusion.

Allowing for luminal diffusion along the length of the capillary, the mass balance equation for the test solute is:

$$\frac{\partial C_L}{\partial t} = D_\infty \frac{\partial^2 C_L}{\partial x^2} - \frac{2k_s}{R}(C_L - C_B) \qquad \text{(A1)}$$

where t is time and x is position along the capillary, with $x = 0$ at the vascular pole (The other symbols are as defined previously in connection with equations 1–4). Equation A1 is the same as equation 1, except for the new term ($D_\infty \partial^2 C_L/\partial x^2$), which accounts for axial diffusion. Both equations assume that radial diffusion within the lumen is relatively rapid, so that concentration variations between the center of a capillary and the wall are negligible. This assumption is justified both

by the observed pattern of luminal fluorescence and by order of magnitude estimates of radial concentration gradients.

To simulate a diffusion experiment, the initial condition and boundary conditions for equation A1 are:

$$C_L = C_0 + C_B \text{ at } t = 0, x > 0 \quad \text{(A2)}$$

$$C_L = C_B \text{ at } x = 0, t > 0 \quad \text{(A3)}$$

$$\frac{\partial C_L}{\partial x} = 0 \text{ at } x = \infty, t > 0 \quad \text{(A4)}$$

Equation A2 states that when the bath is changed at $t = 0$, C_L initially exceed C_B by an amount C_0 (as used before in obtaining equation 2). At all times, the luminal concentration at the vascular pole is assumed to equal that in the bath, as indicated by equation A3. Equation A4 embodies the assumption that for an experiment of moderate duration, there will be positions along a capillary far enough from the vascular pole that axial concentrations gradients will not yet have been created by leakage at the vascular pole. This is consistent with the well-known fact that a finite time is required for diffusional disturbances in concentration fields to propagate over a specified distance.

Equations A1–A4 can be solved using the method of similarity to give:

$$\frac{\Delta C}{C_0} = \exp\left(-\frac{2k_s}{R}t\right) \operatorname{erf}\left(\frac{x}{2\sqrt{D_\infty t}}\right), \quad \text{(A5)}$$

where erf is the error function (33). If the error function were equal to unity, then equation A5 would be equivalent to equations 2 or 3, the solution to the mass balance equation that neglects axial diffusion. The larger its argument, the closer is the error function to unity.

Suppose now that k_s is to be determined from the slope of a plot of $\ln(\Delta C/C_0)$ vs t for $t_1 \le t \le t_2$. Ignoring axial diffusion, we would obtain:

$$k_s = \frac{R}{2}\frac{\ln(\Delta C_1/\Delta C_2)}{t_2 - t_1}, \quad \text{(A6)}$$

where ΔC_i is the concentration difference at $t = t_i$. Including the effects of axial diffusion, we obtain from equation A5

$$k_s^* = \frac{R}{2}\frac{\ln(\Delta C_1/\Delta C_2) - \ln(\operatorname{erf}_1/\operatorname{erf}_2)}{t_2 - t_1}, \quad \text{(A7)}$$

where k_s^* is the "exact" value of the permeability and erf_i is the error function evaluated at $t = t_i$. From equations A6 and A7.

$$k_s^* = k_s - \frac{R}{2}\frac{\ln(\operatorname{erf}_1/\operatorname{erf}_2)}{t_2 - t_1} \quad \text{(A8)}$$

Equation A8 provides a means to calculate the extent to which k_s overestimates the true permeability k_s^*, as a consequence of neglecting axial diffusion.

The value of x that should be used in the error calculation is the path length for luminal diffusion from the site of observation to the vascular pole. If the glomerular tuft is visualized as a globe, and if the cut ends of the arterioles are taken to be located at the south pole, then a representative observation site might be at the equator. In fact, because scans which exhibited a change in C_B were discarded, and because such changes probably reflected a proximity to the vascular pole (southern hemisphere locations), most of the observation sites were probably in the northern hemisphere. Thus, error estimates based on the equator will tend to be conservative. If the overall diameter is d, the shortest (straight line) distance from the equator to a pole is $d/\sqrt{2} = 0.71\,d$, and length of the shortest surface arc is $\pi d/4 = 0.79\,d$. Because of the tortuosity of the capillary network, the actual contour length of the path for axial diffusion should be considerably larger than these values. We chose $x = d$ for the calculations, which is probably conservative.

For unfixed glomeruli isolated from rats of similar size, the average diameter was 220 μm. The radius of the intact capillaries studied averaged 3.4 μm, while that of the acellular capillaries averaged 3.7 μm. For the intact capillaries, the data used to determine the slope were typically from a period beginning at 150 s and ending at 350 s after the change in bath composition. The beginning and ending times for the acellular glomeruli were usually ~ 30 and 75 s, respectively. Using these estimates for x, R, t_1, and t_2 in equation A8, along with the values for D_∞ and k_s already given, we calculate that k_s exceeded k_s^* by ~ 11% for the intact capillaries and by ~ 0.1% for the acellular capillaries. For the reasons already mentioned, these error estimates are probably conservative. We conclude that the error introduced by ignoring axial diffusion is negligible.

Acknowledgments

We wish to thank Dr. B. D. Myers for providing the HPLC equipment for the dextran chromatographic separations, and Rene Brandt and Tracey Martin for excellent technical assistance. We acknowledge the support of the American Heart Association, Minnesota affiliate, and the National Institutes of Health DK 20368 (W. M. Deen) and DK 31437 (T. H. Hostetter).

References

1. Brenner, B. M., M. P. Bohrer, C. Baylis, and W. M. Deen. 1977. Determinants of glomerular permselectivity: insights derived from observations in vivo. *Kidney Int.* 12:229–237.

2. Deen, W. M., C. R. Bridges, and B. M. Brenner. 1983. Biophysical basis of glomerular permselectivity. *J. Membr. Biol.* 71:1–10.

3. Dworkin, L. D., and B. M. Brenner. 1985. Biophysical basis of glomerular filtration. *In* The Kidney: Physiology and Pathophysiology. D. W. Seldin and G. Giebisch, editors. Raven Press, New York. 397–425.

4. Deen, W. M., J. L. Troy, C. R. Robertson, and B. M. Brenner. 1973. Dynamics of glomerular ultrafiltration in the rat. IV. Determination of the ultrafiltration coefficient. *J. Clin. Invest.* 52:1500–1508.

5. Tucker, B. J., and R. C. Blantz. 1981. Effects of glomerular filtration dynamics on the glomerular permeability coefficient. *Am. J. Physiol.* 240(*Renal Fluid Electrolyte Physiol.* 9):F245–F254.

6. Remuzzi, A., and W. M. Deen. 1989. Theoretical effects of network structure on glomerular filtration of macromolecules. *Am. J. Physiol.* 257(*Renal Fluid Electrolyte Physiol.* 26):F152–F158.

7. Friedman, S., S. Strober, E. H. Field, E. Silverman, and B. D. Myers. 1984. Glomerular capillary wall function in human lupus nephritis. *Am. J. Physiol.* 246(*Renal Fluid Electrolyte Physiol.* 15):F580–F591.

8. Daniels, B. S., E. B. Hauser, W. M. Deen, and T. H. Hostetter. 1992. Glomerular basement membrane: in vitro studies of water and protein permeability. *Am. J. Physiol.* 262(*Renal Fluid Electrolyte Physiol.* 31):F918–F926.

9. Ligler, F. S., and G. B. Robinson. 1977. A new method for the isolation of renal basement membranes. *Biochim. Biophys. Acta.* 468:327–340.

10. Carlson, E. C. 1987. Morphology of isolated renal tubular and glomerular basement membranes. *In* Renal Basement Membranes in Health and Disease. R. G. Price and B. G. Hudson, editors. Academic Press Ltd., London. p.p. 99–114.

11. Oliver, J. D., S. Anderson, J. L. Troy, B. M. Brenner, and W. M. Deen. 1992. Determination of glomerular size selectivity in the normal rat using ficoll. *J. Am. Soc. Nephrol.* 3:214–228.

12. Mayer, G., R. A. Lafayette, B. D. Myers, and T. W. Meyer. AII blockade restores size-selectivity but not charge-selectivity in remnant glomeruli. *J. Am. Soc. Nephrol.* 2:685 (Abstr.).

13. Myers, B. D., R. G. Nelson, G. W. Williams, P. H. Bennett, S. A. Hardy, R. L. Berg, N. Loon, W. C. Knowler, and W. E. Mitch. 1991. Glomerular function in Pima Indians with noninsulin-dependent diabetes mellitus of recent onset. *J. Clin. Invest.* 88:524–530.

14. Scandling, J. D., and B. D. Myers. 1992. Glomerular size-selectivity and microalbuminuria in early diabetic glomerular disease. *Kidney Int.* 41:840–846.

15. Farquhar, M. G., S. L. Wissig, and G. E. Palade. Glomerular permeability. I. Ferritin transfer across the normal glomerular capillary wall. 1961. *J. Exp. Med.* 113:47–56.

16. Rennke, H. G., R. S. Cotran, and M. A. Ventkatachalam. 1975. Role of molecular charge in glomerular permeability. *J. Cell Biol.* 67:638–646.

17. Kanwar, Y. S. 1984. Biology of disease. Biophysiology of glomerular filtration and proteinuria. *Lab. Invest.* 51:7–21.

18. Bertolatus, J. A., and D. Klinzman. 1991. Macromolecular sieving by

glomerular basement membrane in vitro: effect of polycation or biochemical modifications. *Microvasc. Res.* 41:311–327.

19. Bray, J., and G. B. Robinson. 1984. Influence of charge on filtration across renal basement membrane films in vitro. *Kidney Int.* 25:527–533.

20. Kanwar, Y. S., and L. J. Rosenzweig. 1982. Altered glomerular permeability as a result of focal detachment of the visceral epithelium. *Kidney Int.* 21:565–574.

21. Miller, P. L., J. W. Scholey, H. G. Rennke, and T. W. Meyer. 1990. Glomerular hypertrophy aggravates epithelial cell injury in nephrotic rats. *J. Clin. Invest.* 85:1119–1126.

22. Rodewald, R., and M. J. Karnovsky. 1974. Porous substructure of the glomerular slit diaphragm in the rat and mouse. *J. Cell Biol.* 60:423–433.

23. Shea, S. M., and A. B. Morrison. 1975. A stereological study of the glomerular filter in the rat. *J. Cell Biol.* 67:436–447.

24. Andrews, P. M., and A. K. Coffey. 1983. Cytoplasmic contractile elements in glomerular cells. *Fed. Proc.* 42:3046–3052.

25. Drenckhahn, D., and R. P. Franke. 1988. Ultrastructural organization of contractile and cytoskeletal proteins in glomerular podocytes of chicken, rat, and man. *Lab. Invest.* 59:673.

26. Lea, P. J., M. Silverman, R. Hegele, and M. J. Hollenberg. 1989. Tridimensional ultrastructure of glomerular capillary endothelium revealed by high-resolution scanning electron microscopy. *Microvasc. Res.* 38:296–308.

27. Bankston, P. W., and A. J. Milici. 1983. A survey of the binding of polycationic ferritin in several fenestrated capillary beds: indication of heterogeneity in the luminal glycocalyx of fenestral disphragms. *Microvasc. Res.* 26:36–48.

28. Latta, H., and S. Fligiel. 1985. Mesangial fenestrations, sieving, filtration, and flow. *Lab Invest.* 52:591–603.

29. Levick, J. R., and L. H. Smaje. 1987. An analysis of the permeability of a fenestra. *Microvasc. Res.* 33:233–256.

30. Landis, E. M. 1927. Micro-injection studies of capillary permeability. II. The relation between capillary pressure and the rate at which fluid passes through the walls of single capillaries. *Am. J. Physiol.* 82:217–238.

31. Pappenheimer, J. R., and A. Soto-Rivera. 1948. Effective osmotic pressure of the plasma proteins and other quantities associated with the capillary circulation in the hind-limbs of cats and dogs. *Am. J. Physiol.* 152:471–491.

32. Pinnick, R. V., and Savin, V. J. 1986. Filtration by superficial and deep glomeruli of normovolemic and volume-depleted rats. *Am. J. Physiol.* 250:F86–91.

33. Abramowitz, M., and I. A. Stegun. 1970. Handbook of Mathematical Functions. National Bureau of Standards, Washington, DC. pp. 310–311.